9-2010

Computational Analysis of Missense Mutations Causing Snyder-Robinson Syndrome

Zhe Zhang
Clemson University

Shaolei Teng
Clemson University

Liangjiang Wang
Clemson University

Charles E. Schwartz
Clemson University

Emil Alexov
Clemson University, ealexov@clemson.edu

Published in final edited form as:
Hum Mutat. 2010 September ; 31(9): 1043–1049. doi:10.1002/humu.21310.

Computational analysis of missense mutations causing Snyder-Robinson Syndrome

Zhe Zhang[1,§], **Shaolei Teng**[1,2,§], **Liangjiang Wang**[2,3], **Charles E. Schwartz**[2,3], and **Emil Alexov**[1,*]

[1] Computational Biophysics and Bioinformatics, Department of Physics, Clemson University, Clemson, SC 29634

[2] Department of Genetics & Biochemistry, Clemson University, Clemson, SC 29634

[3] J.C. Self Research Institute of Human Genetics, Greenwood Genetic Center, Greenwood, SC 29646

Abstract

The Snyder-Robinson syndrome is caused by missense mutations in the spermine sythase gene that encodes a protein (SMS) of 529 amino acids. Here we investigate, *in silico*, the molecular effect of three missense mutations, c.267G>A (p.G56S), c.496T>G (p.V132G) and c.550T>C (p.I150T) in SMS that were clinically identified to cause the disease. Single-point energy calculations, molecular dynamics simulations and pKa calculations revealed the effects of these mutations on SMS's stability, flexibility and interactions. It was predicted that the catalytic residue, Asp276, should be protonated prior binding the substrates. The pKa calculations indicated the p.I150T mutation causes pKa changes with respect to the wild type SMS which involve titratable residues interacting with the S-methyl-5'-thioadenosine (MTA) substrate. The p.I150T missense mutation was also found to decrease the stability of the C-terminal domain and to induce structural changes in the vicinity of the MTA binding site. The other two missense mutations, p.G56S and p.V132G, are away from active site and do not perturb its wild type properties, but affect the stability of both the monomers and the dimer. Specifically, the p.G56S mutation is predicted to greatly reduce the affinity of monomers to form a dimer and therefore should have a dramatic effect on SMS function since dimerization is essential for SMS activity.

Keywords

spermine synthase; *SMS*; Snyder-Robinson syndrome; mental retardation; protein stability

INTRODUCTION

Snyder-Robinson syndrome (SRS; MIM# 309583) [Snyder and Robinson, 1969] is an X-linked recessive disease which causes mild-to-moderate mental retardation, osteoporosis, facial asymmetry, thin habitus, hypotonia, and a nonspecific movement disorder [Bas, et al., 2008]. Genetic studies showed that the SRS is caused by defects in the spermine synthase gene (*SMS*; MIM# 300105) [Bas, et al., 2008; Becerra-Solano, et al., 2009; Cason, et al., 2003; de Alencastro, et al., 2008]. Particularly, a splice variant of the SMS gene in males

* Corresponding author Emil Alexov Clemson University Physics Kinard Lab Clemson South Carolina 29634 United States Phone: (864)656-5307 Fax: (864)656-0805 ealexov@clemson.edu.
§These contributed equally to the manuscript

Supporting Information for this preprint is available from the *Human Mutation* editorial office upon request (humu@wiley.com)

from the original Snyder-Robinson family was found that leads to the loss of exon 4, inserts a premature stop codon and results in a truncated protein containing only the first 110 amino acids [Cason, et al., 2003]. A missense mutation at position 56 substituting Gly with Ser c. 267G>A (p.G56S) was reported in the *SMS* gene from a second family with Snyder-Robinson syndrome [de Alencastro, et al., 2008]. It was shown that the p.G56S mutation greatly reduces SMS activity and leads to severe epilepsy and cognitive impairment [de Alencastro, et al., 2008]. Another missense mutation, c.496T>G (p.V132G), in the exon 5 of the *SMS* gene in two Mexican brothers with Snyder–Robinson syndrome was also found [Becerra-Solano, et al., 2009]. Recently a new mutation, c.550T>C (p.I150T), was identified by Schwartz and co-workers (personal communication). Thus, currently three missense mutations in SMS protein and a splice variant in SMS gene are clinically shown to be associated with SRS. However, the molecular mechanism of how these genetic defects cause SRS is still unknown. While the truncated protein resulting from the splice variant of the *SMS* gene is not expected to retain the wild type function of the SMS protein, the molecular effects of the above missense mutations on the SMS function cannot be revealed without performing a detailed analysis. Such an analysis is reported in the present paper.

The SMS protein is an aminopropyltransferase which converts spermidine into spermine and thus is very important for regulating polyamines' concentration in the cell. It has been shown that polyamines play an important role in cell proliferation, differentiation, programmed death and tissue repair [Gerner and Meyskens, 2004]. Polyamine biosynthesis was found to be negatively regulated by some tumor-suppressor genes, such as the adenomatous polyposis coli gene [Erdman, et al., 1999]. The suppression of polyamine levels can increase apoptosis, decrease cell growth, and prevent tumor formation. Thus, understanding the polyamine biosynthetic pathway could reveal important targets for the design of therapeutic agents [Casero and Marton, 2007]. The predominant polyamines found in prokaryotes and eukaryotes are spermidine (SPD) and spermine (SPM). They can act as ligands at multiple sites on DNA, RNA, proteins, phospholipids, and nucleotide triphosphates. In addition, in higher organisms, SPM is required for modulating ion channel activities of certain cells. The loss of SPM has profound effects in mice since deletion of the *SMS* gene results in reduced size, sterile, deaf and has neurological abnormalities, and very short life span [Wu et al., 2008; Mackintosh and Pegg, 2000]. Polyamines synthesis is catalyzed by aminopropyltransferases which include spermidine synthase and SMS. In this process, S-adenosylmethionine decarboxylase (AdoMetDC) provides the aminopropyl donor decarboxylated S-adenosylmethionine (dcAdoMet) for the synthesis of both spermidine and spermine. Particularly, spermine synthase adds aminopropyl group to the N-10 position of SPD to form SPM.

Recently, the 3D structures of human SMS with either spermidine or spermine were experimentally determined [Wu et al., 2008]. Structural analysis combined with site-directed mutagenesis indicated that two residues, Asp201 and Asp276, play a key role in the catalytic reaction. The human SMS forms a dimer of two identical subunits. Each subunit is made of two functional domains: the N-terminal domain which is important for dimerization, and the C-terminal domain which includes an active site for spermine synthesis [Wu et al., 2008]. Interestingly, the N-terminal of SMS is very similar to AdometDC and the C terminal of SMS has structural homology with spermidine synthase [Wu et al., 2008]. It was shown that both domains are enzymatically inactive when expressed separately, but have well defined 3D structures [Wu et al., 2008]. The importance of dimerization for the function of SMS protein was studied using a series of deletion mutants. It was demonstrated that the N-domain causes dimerization and without dimerization the SMS losses its activity [Wu et al., 2008].

Genetic variations or defects can affect the function of the cell and the function of the corresponding protein in many different ways (see for example) [Dobson, et al., 2006; Karchin, et al., 2005a; Karchin, et al., 2005b; Reumers, et al., 2006; Riva and Kohane, 2002; Teng, et al., 2008; Yue, et al., 2006]. In this study, we investigate three missense mutations (Fig. 1) clinically shown to cause Snyder-Robinson syndrome by the means of computational modeling of their effect on stability, dynamics and function of the SMS dimeric protein. The goal is to reveal the molecular mechanism of the effects, which will provide guidance for further studies toward developing treatment of the disease.

MATERIALS AND METHODS

Protein structures

The wild type (WT) structures of human SMS protein crystallized with either spermidine (PDB ID 3C6K) or spemine (PDB ID 3C6M) [Brooks, et al., 2009] were downloaded from the Protein Data Bank (PDB) website [Kouranov, et al., 2006]. In both cases the asymmetrical unit was found to have four molecules, while the biological unit is a dimer. The dimer made of chains “A” and “B” was found to have many van der Waals (vdW) clashes and was removed from the calculations. Instead, the biological unit was taken as the dimer made of chains “C’ and “D”. There are minor differences between 3C6K and 3C6M structures due to different ligands (spermidine and spermine) and different crystallographic groups (P1 and $P3_2$). However these differences are negligibly small at the dimer interface. Most of the calculations reported in this paper were done using the 3C6M structure because a significant part of the N-terminal domain is not solved in the 3C6K structure. However, the pKa calculations involving mutations at site 150 were done using both 3C6K and 3C6M structures because site 150 is located in close proximity to the active site residues and to the spermidine/spermine binding pocket and even very small structural difference could have significant impact on the calculations.

The mutant structures were built *in silico* by side chain replacement done with the program SCAP [Xiang and Honig, 2001]. Three mutant structures per wild type protein were generated, each corresponding to a mutation introduced at the 56, 132 or 150 sites (Fig. 1) and introducing the clinically observed mutations (p.G56S, p.V132G and p.I150T).

Energy calculations

To reduce the computational time, the structures were split into N-terminal domain (a.a. 1-125) and C-terminal domain (a.a. 126-381), the last one including the central domain as well. The corresponding dimer and the separated monomer structures were energy minimized with the TINKER package [Ponder, 1999] using the “minimize.x” module which performs energy minimization using the Limited Memory BFGS Quasi-Newton Optimization algorithm [Ponder, 1999]. The solvent was modeled using the Still Generalized Born model [Still, et al., 1990] and the internal dielectric constant was set to 1.0. The minimization was done using four different force field parameters Charmm19, Charmm27 [Brooks, et al., 2009], Amber 98 [Case, et al., 2005] and OPLS [Jorgensen and Tirado-Rives, 1988] to test the sensitivity of the results. The convergence criteria applied was RMS gradient per atom = 0.01. After successful energy minimization, the energies of the minimized structures were obtained with “analyze.x” module of TINKER. If not specifically indicated, in this work we focus on the total potential energy. The ligands, S-methyl-5'-thioadenosine: MTA, and SPM/SPD were not included in the energy calculations because neither of the mutation sites are in direct contact with any of them.

The binding energy ($\Delta\Delta G$(binding)) was calculated as the difference between the total potential energy of the dimer minus the total potential energy of the separated monomers,

$$\Delta\Delta G\,(binding) = \Delta G\,(\text{dimer}) - \Delta G\,(C) - \Delta G\,(D)\,, \tag{1}$$

where ΔG(dimer) is the potential energy of the dimer, ΔG(C) and ΔG(D) are the potential energies of monomer "C" and "D", respectively. These calculations were done for WT structures and for each mutant and the difference, which evaluates the effect of the mutation on the affinity (binding), was calculated as [Teng, et al., 2009a]:

$$\Delta\Delta\Delta G\,(mut) = \Delta\Delta G\,(binding \quad :WT) - \Delta\Delta G\,(binding \quad :\text{mutant}) \tag{2}$$

where $\Delta\Delta G(binding : WT)$ is the binding energy of the WT monomers and $\Delta\Delta G(binding :$ mutant) is the binding energy of the corresponding mutant. The above equations (1,2) assume that the entropy change associated with the dimer formation is practically the same for the WT and mutant and thus cancels out.

The effect of the mutations on the stability (folding energy) of individual monomers was modeled by the following protocol. The total potential energy of each separated monomer was obtained with TINKER. In addition, a seven residue segment centered at the mutation site was taken from the original structures. Then the folding energy was calculated as:

$$\Delta G\,(folding) = G\,(folded) - G\,(unfolded) = G\,(folded) - G_0\,(unfolded) - G_7\,(unfolded) \tag{3}$$

where *G(folded)* is the total potential energy calculated with the corresponding minimized 3D structure using the analyze.x module of TINKER, and *G(unfolded)* is the energy of unfolded state. The unfolded state energy is further split into G_0(unfolded) and G_7(unfolded). The second term is calculated as explained above on a seven residue segment (different segment lengths were explored, but no effect was found up to nine), while the first term is considered to be mutation independent and cancels out in eq. (4). Thus, the effect of a mutation is calculated as:

$$\begin{aligned}\Delta\Delta G\,(folding\_mut) &= \Delta G\,(folding \quad :WT) \\ &\quad - \Delta G\,(folding \quad :mutation) \\ &= G\,(folded \quad :WT) \\ &\quad - G_7\,(unfolded \quad :WT) \\ &\quad - G\,(folded \quad :mutation) \\ &\quad + G_7\,(unfolded \quad :mutation)\end{aligned} \tag{4}$$

Such an approach of calculating the effect of mutations on the folding energy assumes that the unfolded state of the WT and mutant are similar and the main difference is around the site of mutation and there are no residual interactions between the site of mutation and amino acids further away than three positions along the sequence. Although this is an approximation, such an approach was shown to provide very good correlation to experimental data of the effect of mutation on the melting temperature [Ofiteru, et al., 2007].

pKa calculations

The motivation for performing *pKa* calculations to reveal the effect of mutations on the ionization states of titratable groups comes from the observation that even mutations that do

not involve titratable groups may affect ionization states by perturbing the original dielectric boundary of the protein or by altering the hydrogen bond network [Talley, et al., 2008; Teng, et al., 2009a]. Thus, while clinically observed missense mutations involve no titratable group, still they can affect the *pKa's* of their neighbors.

The p*Ka* values of the ionizable groups were calculated using the Multi Conformation Continuum Electrostatics (MCCE) method as previously described [Alexov, 2003; Alexov and Gunner, 1997; Georgescu, et al., 2002]. Default parameters were used as protein dielectric constant of 8.0 and ionic strength of 0.15M. Because the pKa values of titratable groups are known to be affected by mutations at distant sites, the ligands (S-methyl-5'-thioadenosine: MTA, spermidine: SPD and spermine: SPM) were included in the MCCE calculations in case of wild type (WT) and p.I150T mutant. The MCCE topology files were obtained following Refs. [Kleywegt, 2007; Kleywegt, et al., 2003; Kleywegt and Jones, 1998; Lau and Bruice, 2000] and are provided in the Supporting Information. This resulted in the following net charges: spermine = +4e, spermidine = +3e and MTA = +1e. The charges of the ligands were kept fixed during MCCE calculations.

Calculations were performed on the WT dimer and separated monomers (using both 3C6K and 3C6M structures) as well on all mutants. The calculated *pKa* of the ith amino acid using WT structure (either dimer or separate monomers) and the corresponding mutant structures was compared as:

$$\Delta pK_i\,(mut) = pKa_i\,(WT) - pKa_i\,(mutation) \tag{5}$$

where $pKa_i(WT)$ is the *pKa* of amino acid "i" calculated with the WT structure and $pKa_i(mutation)$ is the *pKa* of the same amino acid but calculated using mutant structure.

Web servers

Several of web-based tools were used to predict the effect of the missense mutations on SMS stability and dimer affinity. The list is provided in the Supporting Information and they are described in the following Refs. [Capriotti, et al., 2005; Lu, et al., 2009; Parthiban, et al., 2006; Schymkowitz, et al., 2005; Teng, et al., 2009b; Teng, et al., 2010; Yin, et al., 2007].

RESULTS

A previous study based on the X-ray structures of spermine synthase with either spermidine or spermine has found the catalytic residues, residues being in contact with the substrates/products and amino acids conserved in the multiple sequence alignment (see Fig.3 in Ref. [Wu et al., 2008]) and we will take advantage of their analysis. The study [Wu et al., 2008] revealed several crucial structural and biochemical characteristics governing the wild type function of SMS. These findings are grouped in four categories for the purposes of the present investigation: (a) The reaction follows the standard mechanism of aminopropyltransferases and involves cleavage of a peptide bond and deprotonation of the N-10 atom of spermidine [Ikeguchi, et al., 2006; Pegg and Michael, 2009]. Thus, protonation/deprotonation events are crucial for spermine synthase function and motivated us to perform a detailed analysis of the pKa's of titratable residues at different conditions. (b) The reaction requires precise positioning of both the reactants and products in the active site of the SMS. The positions of the substrates are coordinated by the set of amino acids reported in the original paper [Wu et al., 2008]. Any structural perturbation that alter the geometry of the active site or side chain positions of coordinating residues would affect the reaction. (c) The reaction takes place inside the SMS, where both reactants are buried and shielded from the water phase. Any change of the stability or conformational dynamics

involving structural segments surrounding the active sites would affect the reaction. (d) The dimerization of SMS was shown to be crucial for the function and any mutation that alters the SMS dimer stability is expected to alter the function as well. Below we investigate the effect of three clinically observed missense mutations on each of the above mentioned properties (see Fig.1 showing mutation sites locations).

Effect of the missense mutations on ionization states of titratable groups

The first question to address is which titratable groups are affected by the binding of reactants. Since no 3D structure is available of the apo form of SMS, we performed pKa calculations using 3C6K and 3C6M structures without substrates as a model of the apo form. This is an obvious simplification, since both structures are “closed” structures, i.e. the reactants binding pockets are shielded from the water phase, while the apo conformation is expected to have channel(s) leading the reactants to their binding positions. However, in the pKa calculations, the binding pockets were empty and treated as medium of high dielectric constant of water and thus the amino acids within the binding pockets are exposed to the water phase as they are supposed to be in the apo form. Of course, titratable groups located away from the binding pockets and within structural regions that undergo conformation changes from apo to holo states will experience pKa shifts, but these groups are not the subject of the present study, neither the amino acids in the N-terminus domain of the SMS.

The results of pKa calculations are summarized in Table 1. With respect to the wild type SMS, it was found that the catalytic residues Asp201(203) and Asp276(278) behave differently (in parenthesis are given the amino acid numbers in the 3C6K structure). The Asp201 is calculated to be fully ionized with and without substrates, while the Asp276 is predicted to be protonated without substrates but to be fully ionized when they are present. This is a confirmation of the catalytic mechanism outlined in references [Wu et al., 2008;Pegg and Michael, 2009]. The Asp276 serves as proton acceptor that removes a proton from the N-10 atom of spermidine and in order to do so, must have an elevated pKa prior the attack. The Glu353(355) was also found to have an elevated pKa prior SPD/SPM binding, but becomes fully ionized in the presence of substrates. However, the ionization state of neither of these residues is affected by the p.I150T mutation, because they are far away from residue 150. Two amino acids within the MTA binding pocket were calculated to experience pKa shifts due to MTA binding and the p.I150T mutation (Table 1). The Glu220(222) is calculated to be partially protonated in absence of MTA, mostly because its side chain is partially buried in the protein matrix and the ionized form has to pay a desolvation penalty for that. The binding of MTA, however, provides favorable interactions, supports the ionized form and makes Glu220 fully ionized. The carboxyl oxygens of Glu220 serve as proton acceptors for the OH group of MTA and thus lock the MTA in desired position. The Asp222(224) is not in direct contact with MTA, but interacts electrostatically with Glu220. In the wild type SMS, Asp222 makes a strong hydrogen bond with Ser145(147) and is predicted to be fully ionized and have a low pKa value. The missense mutation at site 150 replaces Ile with Thr, a polar residue which is a strong hydrogen donor. We predict that in the mutant, the OD1 atom of the side chain of Asp222 establishes a new hydrogen bond with Thr150 (Fig. 2c) and this additionally lowers its pKa value. As a “domino effect”, the pKa value of Glu220, which coordinates MTA, gets slightly higher which could affect its interactions with MTA. As result of the p.I150T missense mutation, the hydrogen bond network in the vicinity of the MTA binding site is altered with respect to the wild type, which in turn could affect the reaction.

The other two missense mutations, p.G56S and p.V132G were found not to affect any ionization state, simply because the mutation sites are located in regions that do not have titratable residues around.

Effect of mutations on the stability of the monomers

Structure-based energy calculations were performed as explained in the method section and MTA and SPM were not included in the analysis, the reason being three fold: (a) the missense mutations p.G56S and p.V132G are far away from the binding pockets and thus should not be sensitive to the presence of substrates; (b) the holo (substrate loaded) structure is expected to be much more rigid and stable than the apo structure and thus less sensitive to missense mutations studied in this work and (c) most of the web-based tools do not include substrates in their analysis and to compare their predictions with ours we prefer not to include substrates in our analysis either.

Structure-based energy calculations

The results are summarized in Table 2. The first observation is that the absolute value of the energy change varies depending on the force field parameters and polypeptide chains used, an observation that confirms our previous investigations [Talley, et al., 2008]. However, averaging over all calculated energy changes results in a prediction that all mutations will destabilize monomers. The most prominent is the effect calculated for p.I150T mutation, and the smallest effect is predicted for p.V132G mutation.

Predictions made with web-based tools

The predictions of web-based tools are shown in Table 3 for each missense mutation studied in this work. The most controversial predictions are made with CUPSAT, where the effect on denaturant stability is predicted to be just opposite to the effect on thermal stability. The only other discrepancy among the predictions is the p.G56S missense mutation effect predicted with Eris, which is calculated to slightly increase the monomer stability. However, the consensus among the methods, including sequence based predictions, is that all mutations will decrease monomer's stability.

Structural origin of predicted effects

Comparing results of the structure-based energy calculations with TINKER and web-based tools, we see that they are in very good agreement for all mutations. Almost all methods predict that the mutations will destabilize SMS monomers as our TINKER analysis suggests as well. The predictions obtained with CUPSAT are the most ambiguous, since the effect of thermal and denaturant stabilities are calculated to be just opposite. Without focusing on this discrepancy, which is associated with CUPSAT algorithm, below we discuss plausible structural factors causing the stability changes.

The p.G56S mutation is evaluated by our calculations, all sequence-based and most of the structure-based servers to destabilize the monomers. The wild type residue, the Gly, is frequently found to be located at structural positions requiring either flexibility or sharp turn. Substitution of Gly to Ser residue causes structural reorganization (Fig. 2a) of a neighboring loop consisting of residues Tyr89-Gln94, which in turn affects the beginning of the corresponding helix. Such a structural change induces extra strain and destabilizes SMS monomer.

The p.V132G mutation is predicted by all methods (excluding CUPSAT(denat)) to destabilize 3D structures of the monomers. The structural origin for such predictions is shown in Fig. 2b. The WT residue, Val, is partially buried in the monomers and fully buried in the dimer (shown in green in Fig. 2b). Being hydrophobic amino acid, the WT Val stabilizes the 3D structure due to the hydrophobic effect. The missense mutation introduces Gly, an amino acid that does not have the same hydrophobicity as Val and is smaller as well. As results, the stability of the monomer decreases upon p.V132G mutation. The mutation

also induces small structural changes mostly associated with neighboring side chains, while the backbone is practically unaffected.

The p.I150T mutation is predicted by our calculations to destabilize the monomers in agreement with the web-based tools. The I150 mutation site is quite different as compared with the other two. The side chain of the wild type and the mutant residue points toward the hydrophobic core of the protein. The mutation introduces a polar residue (Thr) which has to pay a significant desolvation penalty to be buried. However, in our protocol it relaxes structurally and establishes a hydrogen bond with Asp222 (Fig. 2c). It should be mentioned as well that the p.I150T mutation causes structural reorganization of a loop made of residues Leu221-Lys260. This is the largest structural change found to be induced by any of the three missense mutations. Since it involves structural segment that is within vicinity of MTA binding site, these structural changes can be expected to affect the wild type function of SMS.

Effect on dimer affinity

The p.G56S mutation is predicted to significantly reduce affinity of monomers to form a dimer, in agreement with FoldX (Table 4). The reason for that is the structural reorganization shown in Fig. 2a, which in turn affects the interactions across dimer interface. The p.V132G mutation is predicted by our protocol to have little effect on affinity, while FoldX calculates almost 3kcal/mol reduction. The reason for such a difference is that we allow for extensive structural relaxation which significantly eases any sterical clashes and minimizes unfilled cavities. In addition, the analysis of the structure (Fig. 2b) shows that the side chain of the wild type residue (Val) does not point toward the dimer interface but it is parallel to it. Because of that Val→Gly mutation is predicted to have little effect of dimerization. The p.I150T mutation is predicted by us and FoldX not to affect dimerization. This is to be expected, since mutation site is far away form the dimer interface. Structural changes induced by p.I150T mutation propagate to the dimer interface; however, they are small and cause almost no effect.

DISCUSSION

Three missense mutations, clinically shown to cause Shyder-Robinson syndrome were investigated to reveal the details of the molecular mechanism causing the disease. This was possible due to recently solved 3D structure of the SMS dimer in presence of either SPD or SPM [Wu et al., 2008]. The 3D structures were subjected to pKa calculations, energy calculations and MD simulations. The analysis was complemented with simultaneous predictions made with web-based resources and the results were compared. Two distinctive mechanisms were found which the missense mutations studied in this work utilize in order to perturb the wild type properties of the SMS. Here we use the word “perturbation” to refer to any change of the wild type characteristics of SMS, since the disease could be caused not only by destabilization of the 3D structure. There are many examples of single nucleotide polymorphism that were shown to increase the stability of either RNA [Capon, et al., 2004] or the corresponding protein [Allali-Hassani, et al., 2009; Schickel, et al., 2007] and to enhance protein-protein interactions [Teng, et al., 2009a]. The same argument can be made for any other SMS property, which if altered from its wild type characteristics, could result in a pathogenic effect [Lupo, et al., 2009; Najat, et al., 2009] or natural difference [Merino, et al., 2009].

Two of the missense mutations, p.G56S and p.V132G, occur either at the dimer interface (p.V132G) or at its periphery (p.G56S), both far away from the active site residues. They both are predicted to destabilize SMS monomers and p.G56S is also predicted to strongly reduce the affinity of monomers to form a dimer. Since dimerization is crucial for the SMS

function, as shown experimentally [Wu et al., 2008], the change would be affecting SMS function as well. Such missense mutations, that do not affect either the catalytic residues or the geometry of the active site, illustrate the case of missense mutations causing disease through indirect effects that alter the function of the corresponding protein.

The third mutation, the p.I150T, is located within the C-terminal domain which carries the active site and is responsible for SPD synthesis. However, neither the wild type Ile150 nor the mutant residue Thr150 are in direct contact with either catalytic amino acids or substrates. However, our analysis revealed that a plausible scenario may involve a “domino effect”, such that the mutant residue, Thr150, makes a hydrogen bond with a neighboring titratable residue, Asp222, which in turn interacts with Asp220, the amino acid that coordinates MTA (and presumably coordinates the natural substrate as shown in Ref. [Wu et al., 2008]). It could be envisioned that altering the wild type interactions, which involve amino acids within the active site, would affect SMS function and could be the cause of the disease. In addition, comparing snapshot of WT and mutant, we found that a structural region involving Asp220 changes its conformational dynamics due to the mutation. The last, but not the least observation, is that the mutation site, I150, is within the same beta strand as another active site residue, Gln148. Altering Gln148 position would affect MTA binding and definitely would affect the SMS reaction. Thus, the p.I150T mutation utilizes several different mechanisms to alter SMS function, but they all affect active site residues, which illustrate the case of a missense mutation causing a direct effect.

It should be pointed out that our computational analysis is not aimed at predicting the absolute value of the expected energy changes, but rather to predict their direction (stabilizing or destabilizing) and more importantly to reveal the details of the suggested changes. This is the major advantage of structure-based approaches, because they show the details of the changes causing the malfunction of the corresponding protein and in principle these findings could be used to develop therapeutics to neutralize the effect. In addition, our investigation provides testable predictions about the effects of the mutations on stability of the monomers and SMS dimer. The predicted tendencies could be tested by the means of thermal or denaturant unfolding experiments and the calculated increase of flexibility of the structural segment comprised of residues 221-260 due to p.I150T mutation could be studied by NMR or other methods. The pKa changes and hydrogen bond rearrangement predicted to occur due to p.I150T substitution could also be assessed by NMR as well as by titration experiments.

Supplementary Material

Refer to Web version on PubMed Central for supplementary material.

Acknowledgments

This work was supported by the National Institutes of Health, grant number 1R03LM009748 to E.A. The support of Clemson University CCIT group, especially Corey Ferrier, is greatly appreciated. Dedicated to the memory of Ethan Francis Schwartz (1996-1998).

REFERENCES

Alexov E. Role of the protein side-chain fluctuations on the strength of pair-wise electrostatic interactions: comparing experimental with computed pK(a)s. Proteins. 2003; 50(1):94–103. [PubMed: 12471602]

Alexov E, Gunner M. Incorporating Protein Conformation Flexibility into the Calculation of pH-dependent Protein Properties. Biophysical Journal. 1997; 74:2075–2093. [PubMed: 9129810]

Allali-Hassani A, Wasney GA, Chau I, Hong BS, Senisterra G, Loppnau P, Shi Z, Moult J, Edwards AM, Arrowsmith CH, Park HW, Schapira M, Vedadi M. A survey of proteins encoded by non-synonymous single nucleotide polymorphisms reveals a significant fraction with altered stability and activity. Biochem J. 2009; 424(1):15–26. [PubMed: 19702579]

Bas DC, Rogers DM, Jensen JH. Very fast prediction and rationalization of pKa values for protein-ligand complexes. Proteins. 2008; 73(3):765–83. [PubMed: 18498103]

Becerra-Solano LE, Butler J, Castaneda-Cisneros G, McCloskey DE, Wang X, Pegg AE, Schwartz CE, Sanchez-Corona J, Garcia-Ortiz JE. A missense mutation, p.P.V132G, in the X-linked spermine synthase gene (SMS) causes Snyder-Robinson syndrome. Am J Med Genet A. 2009; 149A(3):328–35. [PubMed: 19206178]

Brooks BR, Brooks CL 3rd, Mackerell AD Jr. Nilsson L, Petrella RJ, Roux B, Won Y, Archontis G, Bartels C, Boresch S, Caflisch A, Caves L, Cui Q, Dinner AR, Feig M, Fischer S, Gao J, Hodoscek M, Im W, Kuczera K, Lazaridis T, Ma J, Ovchinnikov V, Paci E, Pastor RW, Post CB, Pu JZ, Schaefer M, Tidor B, Venable RM, Woodcock HL, Wu X, Yang W, York DM, Karplus M. CHARMM: the biomolecular simulation program. J Comput Chem. 2009; 30(10):1545–614. [PubMed: 19444816]

Capon F, Allen MH, Ameen M, Burden AD, Tillman D, Barker JN, Trembath RC. A synonymous SNP of the corneodesmosin gene leads to increased mRNA stability and demonstrates association with psoriasis across diverse ethnic groups. Hum Mol Genet. 2004; 13(20):2361–8. [PubMed: 15333584]

Capriotti E, Fariselli P, Casadio R. I-Mutant2.0: predicting stability changes upon mutation from the protein sequence or structure. Nucleic Acids Res. 2005; 33(Web Server issue):W306–10. [PubMed: 15980478]

Case DA, Cheatham TE 3rd, Darden T, Gohlke H, Luo R, Merz KM Jr. Onufriev A, Simmerling C, Wang B, Woods RJ. The Amber biomolecular simulation programs. J Comput Chem. 2005; 26(16): 1668–88. [PubMed: 16200636]

Casero RA Jr. Marton LJ. Targeting polyamine metabolism and function in cancer and other hyperproliferative diseases. Nat Rev Drug Discov. 2007; 6(5):373–90. [PubMed: 17464296]

Cason AL, Ikeguchi Y, Skinner C, Wood TC, Holden KR, Lubs HA, Martinez F, Simensen RJ, Stevenson RE, Pegg AE, Schwartz CE. X-linked spermine synthase gene (SMS) defect: the first polyamine deficiency syndrome. Eur J Hum Genet. 2003; 11(12):937–44. [PubMed: 14508504]

de Alencastro G, McCloskey DE, Kliemann SE, Maranduba CM, Pegg AE, Wang X, Bertola DR, Schwartz CE, Passos-Bueno MR, Sertie AL. New SMS mutation leads to a striking reduction in spermine synthase protein function and a severe form of Snyder-Robinson X-linked recessive mental retardation syndrome. J Med Genet. 2008; 45(8):539–43. [PubMed: 18550699]

Dobson RJ, Munroe PB, Caulfield MJ, Saqi MA. Predicting deleterious nsSNPs: an analysis of sequence and structural attributes. BMC Bioinformatics. 2006; 7:217. [PubMed: 16630345]

Erdman SH, Ignatenko NA, Powell MB, Blohm-Mangone KA, Holubec H, Guillen-Rodriguez JM, Gerner EW. APC-dependent changes in expression of genes influencing polyamine metabolism, and consequences for gastrointestinal carcinogenesis, in the Min mouse. Carcinogenesis. 1999; 20(9):1709–13. [PubMed: 10469614]

Georgescu R, Alexov E, Gunner M. Combining Conformational Flexibility and Continuum Electrostatics for Calculating Residue pKa's in Proteins. Biophysical Journal. 2002; 83:1731–1748. [PubMed: 12324397]

Gerner EW, Meyskens FL Jr. Polyamines and cancer: old molecules, new understanding. Nat Rev Cancer. 2004; 4(10):781–92. [PubMed: 15510159]

Ikeguchi Y, Bewley MC, Pegg AE. Aminopropyltransferases: function, structure and genetics. J Biochem. 2006; 139(1):1–9. [PubMed: 16428313]

Jorgensen WL, Tirado-Rives J. The OPLS potential function for proteins. J. Am. Chem. Soc. 1988; 110:1657–1666.

Karchin R, Diekhans M, Kelly L, Thomas DJ, Pieper U, Eswar N, Haussler D, Sali A. LS-SNP: large-scale annotation of coding non-synonymous SNPs based on multiple information sources. Bioinformatics. 2005a; 21(12):2814–20. [PubMed: 15827081]

Karchin R, Kelly L, Sali A. Improving functional annotation of non-synonomous SNPs with information theory. Pac Symp Biocomput. 2005b:397–408.

Kleywegt GJ. Crystallographic refinement of ligand complexes. Acta Crystallogr D Biol Crystallogr. 2007; 63(Pt 1):94–100. [PubMed: 17164531]

Kleywegt GJ, Henrick K, Dodson EJ, van Aalten DM. Pound-wise but penny-foolish: How well do micromolecules fare in macromolecular refinement? Structure. 2003; 11(9):1051–9. [PubMed: 12962624]

Kleywegt GJ, Jones TA. Databases in protein crystallography. Acta Crystallogr D Biol Crystallogr. 1998; 54(Pt 6 Pt 1):1119–31. [PubMed: 10089488]

Kouranov A, Xie L, de la Cruz J, Chen L, Westbrook J, Bourne PE, Berman HM. The RCSB PDB information portal for structural genomics. Nucleic Acids Res. 2006; 34(Database issue):D302–5. [PubMed: 16381872]

Lau E, Bruice T. Comparison of the Dynamics for Ground-State and Transition-State Structures in the Active Site of Catechol O-Methyltransferase. J. Am. Chem. Soc. 2000; 122(30):7165–7171.

Lu B, Cheng X, Huang J, McCammon JA. An Adaptive Fast Multipole Boundary Element Method for Poisson-Boltzmann Electrostatics. J Chem Theory Comput. 2009; 5(6):1692–1699. [PubMed: 19517026]

Lupo V, Galindo MI, Martinez-Rubio D, Sevilla T, Vilchez JJ, Palau F, Espinos C. Missense mutations in the SH3TC2 protein causing Charcot-Marie-Tooth disease type 4C affect its localization in the plasma membrane and endocytic pathway. Hum Mol Genet. 2009; 18(23): 4603–14. [PubMed: 19744956]

Mackintosh CA, Pegg AE. Effect of spermine synthase deficiency on polyamine biosynthesis and content in mice and embryonic fibroblasts, and the sensitivity of fibroblasts to 1,3-bis-(2-chloroethyl)-N-nitrosourea. Biochem J. 2000; 351(Pt 2):439–47. [PubMed: 11023830]

Merino G, Real R, Baro MF, Gonzalez-Lobato L, Prieto JG, Alvarez AI, Marques MM. Natural allelic variants of bovine ATP-binding cassette transporter ABCG2: increased activity of the Ser581 variant and development of tools for the discovery of new ABCG2 inhibitors. Drug Metab Dispos. 2009; 37(1):5–9. [PubMed: 18824523]

Najat D, Garner T, Hagen T, Shaw B, Sheppard PW, Falchetti A, Marini F, Brandi ML, Long JE, Cavey JR, Searle MS, Layfield R. Characterization of a non-UBA domain missense mutation of sequestosome 1 (SQSTM1) in Paget's disease of bone. J Bone Miner Res. 2009; 24(4):632–42. [PubMed: 19049332]

Ofiteru A, Bucurenci N, Alexov E, Bertrand T, Briozzo P, Munier-Lehmann H, Gilles AM. Structural and functional consequences of single amino acid substitutions in the pyrimidine base binding pocket of Escherichia coli CMP kinase. Febs J. 2007; 274(13):3363–73. [PubMed: 17542990]

Parthiban V, Gromiha MM, Schomburg D. CUPSAT: prediction of protein stability upon point mutations. Nucleic Acids Res. 2006; 34(Web Server issue):W239–42. [PubMed: 16845001]

Pegg AE, Michael AJ. Spermine synthase. Cell Mol Life Sci. 2009

Ponder, JW. Version 3.7. Washington University; St. Luis: 1999. TINKER-software tools for molecular design..

Reumers J, Maurer-Stroh S, Schymkowitz J, Rousseau F. SNPeffect v2.0: a new step in investigating the molecular phenotypic effects of human non-synonymous SNPs. Bioinformatics. 2006; 22(17): 2183–5. [PubMed: 16809394]

Riva A, Kohane IS. SNPper: retrieval and analysis of human SNPs. Bioinformatics. 2002; 18(12): 1681–5. [PubMed: 12490454]

Schickel J, Pamminger T, Ehrsam A, Munch S, Huang X, Klopstock T, Kurlemann G, Hemmerich P, Dubiel W, Deufel T, Beetz C. Isoform-specific increase of spastin stability by N-terminal missense variants including intragenic modifiers of SPG4 hereditary spastic paraplegia. Eur J Neurol. 2007; 14(12):1322–8. [PubMed: 17916079]

Schymkowitz J, Borg J, Stricher F, Nys R, Rousseau F, Serrano L. The FoldX web server: an online force field. Nucleic Acids Res. 2005; 33(Web Server issue):W382–8. [PubMed: 15980494]

Snyder RD, Robinson A. Recessive sex-linked mental retardation in the absence of other recognizable abnormalities. Report of a family. Clin. Pediatr. 1969; 8:669–674.

Still WC, Tempczyk A, Hawley RC, Hendrickson T. Semianalytical Treatment of Solvation for Molecular Mechanics and Dynamics. Journal of the American Chemical Society. 1990; 112:6127–6129.

Talley K, Ng K, Shroder M, Kundrotas P, Alexov E. On the electrostatic component of the binding free energy. PMC Biophysics. 2008; (1):2. [PubMed: 19351424]

Teng S, Madej T, Panchenko A, Alexov E. Modeling effects of human single nucleotide polymorphisms on protein-protein interactions. Biophys J. 2009a; 96(6):2178–88. [PubMed: 19289044]

Teng S, Michonova-Alexova E, Alexov E. Approaches and resources for prediction of the effects of non-synonymous single nucleotide polymorphism on protein function and interactions. Curr Pharm Biotechnol. 2008; 9(2):123–33. [PubMed: 18393868]

Teng, S.; Srivastava, AK.; Wang, L. 2009b. Teng, S.; Srivastava, AK.; Wang, L. Biological Features for Sequence-Based Prediction of Protein Stability Changes upon Amino Acid Substitutions.. Proceedings of the 2009 International Joint Conference on Bioinformatics, Systems Biology and Intelligent Computing (IJCBS'09); 2009. p. 201-206.IEEE Computer Society. Proceedings of the 2009 International Joint Conference on Bioinformatics, Systems Biology and Intelligent Computing (IJCBS'09); p. 201-206.

Teng S, Srivastava AK, Wang L. Sequence feature-based prediction of protein stability changes upon amino acid substitutions. BMC Genomics. 2010 in press.

Wu H, Min J, Zeng H, McCloskey DE, Ikeguchi Y, Loppnau P, Michael AJ, Pegg AE, Plotnikov AN. Crystal structure of human spermine synthase: implications of substrate binding and catalytic mechanism. J Biol Chem. 2008; 283(23):16135–46. [PubMed: 18367445]

Xiang Z, Honig B. Extending the Accuracy Limits of Prediction for Side-chain Conformations. J. Mol. Biol. 2001; 311:421–430. [PubMed: 11478870]

Yin S, Ding F, Dokholyan NV. Eris: an automated estimator of protein stability. Nat Methods. 2007; 4(6):466–7. [PubMed: 17538626]

Yue P, Melamud E, Moult J. SNPs3D: candidate gene and SNP selection for association studies. BMC Bioinformatics. 2006; 7:166. [PubMed: 16551372]

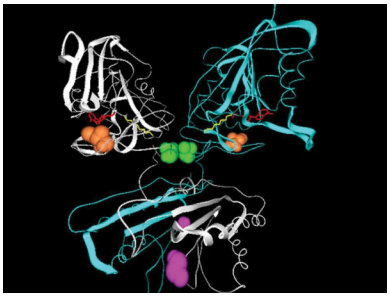

Fig. 1.

The 3D structure of SMS dimer in ribbon representation using “C’ (blue) and “D” (while) chains of 3C6K structure. The MTA is shown in red and SPD in yellow. The mutation sites are shown as: p.G56 (purple), p.V312 (green) and p.I150 (orange).

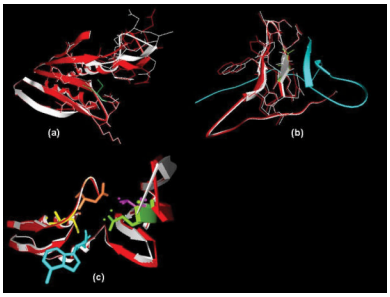

Fig. 2.

Zoomed 3D structure of SMS focused on the corresponding mutation site. The "C" chain of the corresponding minimized mutant structure (white) is superimposed structurally onto wild type minimized "C" chain (red) for comparison. The mutant "D" chain is also shown when applicable to indicate where the interface is.

(a) Zoomed N-terminal domain. Amino acids 1-19 and above 118 are removed to reduce the complexity of the figure. The WT and mutant backbones are shown with ribbons. The side chains of amino acids around 56 mutation site are shown as "wires" and the missense mutation Ser56 is shown in green.

(b) The 3D structure of the SMS dimer (amino acids 120-150), with "C" chain of the wild type (red) and the mutant p.V132G (white) superimposed. The "D" chain of the mutant is shown as blue ribbon. The side chains of the residues within the vicinity of the site of mutation are shown as well and the WT Val is green.

(c) Zoomed C-terminal domain of the p.I150T mutant (white) superimposed onto the wild type structure (red). The mutant residue, Thr150 is shown in magenta, the titratable residue affected by the mutation, Asp222, is shown in orange, the coordinating residues Gln1648 in green and Glu220 in yellow. The MTA in blue. The hydrogen of Thr150 making H-bond with Asp222 and the hydrogens of Gln148 are also shown in the figure.

Table 1

The calculated pKa's of ionizable groups with either SPD/SPM or MTA at the binding pocket

	SPD/SPM pocket			MTA pocket	
	p.D 201/203	**p.D 276/278**	**p.E 353/355**	**p.E 220/222**	**p.D 222/224**
no substrates	0.0 / 5.0	9.6 / 9.7	8.5 / 10.0	6.0 / 6.5	3.0 / 1.4
with substrates	0.0 / 0.0	1.3 / 0.0	0.0 / 0.0	0.2 / 0.0	0.7 / 1.6
p.I150T no substrates	0.0 / 5.0	9.6 / 9.7	8.5 / 10. 0	6.3/7.0	0.2/0.0
p.I150T with substrates	0.0 / 0.0	1.3 / 0.0	0.0 / 0.0	0.3/0.0	0.4/1.4

The calculations were performed with 3C6M and 3C6K structures and results averaged over the “C” and “D” polypeptide chains. The residue numbers are reported for both structures, starting with 3C6M numbers. Four conditions were modeled: pKa calculations without substrates, with substrates and the same was repeated with introduced missense mutation p.I150T. The pKa's of residues at SPD/SPM binding site were found not to be affected by p.I150T mutation, while the pKa's of residues at the vicinity of the MTA pocket were found to be sensitive to the p.I150T mutation.

Hum Mutat. Author manuscript; available in PMC 2011 September 1.

Table 2

The results of structure-based (3C6K) energy calculations

Missense mutation/chain	Charmm-19	Charmm-27	Amber-98	OPLS	Average	Average (C-D chains)
p.G56S – C	2.1	-1.1	0.8	-4.2	-0.6±1.4	-2.8 ± 1.8
p.G56S – D	-1.3	-14.8	-1.8	-2.0	-5.0 ± 3.3	
p.V132G-C	-12.7	-1.0	3.2	5.3	-1.3 ± 4.0	-1.1 ± 2.4
p.V132G-D	-10.6	2.8	-0.1	4.2	-0.9± 3.3	
p.I150T-C	-3.3	-2.3	-9.0	1.3	-3.3±2.1	-3.5 ± 2.4
p.I150T-D	7.5	-4.7	-15.5	-2.3	-3.7 ± 4.7	

Four different force field parameters (Charmm-19, Charmm-27, Amber-98 and OPLS) were used. All energies are in kcal/mol. Negative energy change indicates that the mutation decreases the stability, while positive increases it. The modeling was done using “C” and “D” chains of 3C6K structure independently and then results were averaged. Standard error is reported as well.

Hum Mutat. Author manuscript; available in PMC 2011 September 1.

Table 3

Predictions made with web-based tools

Web-server	p.G56S	p.V132G	p.I150T
CUPSAT (thermal)	+11.53	-4.12	-2.57
CUPSAT (denat.)	-1.45	+7.66	+4.14
Eris	+0.20	-5.27	-4.27
I-Mutant 2.0	-2.1	-3.04	-2.97
FoldX	-3.48	-0.57	-3.32
MUpro	Destabilizing	Destabilizing	Destabilizing
MuStab	Destabilizing	Destabilizing	Destabilizing
Consensus	Destabilizing	Destabilizing	Destabilizing

The results of the structure-based tools are in kcal/mol and negative energy change indicates that the mutation is predicted to destabilize the SMS structure, while positive number suggests the opposite. The results were averaged for “C” and “D” chains. The sequence based servers do not predict the magnitude of the change, but its direction only in terms of stabilizing/destabilizing. The last row provides consensus prediction.

Table 4

The results of structure-based (3C6K) energy calculations on the dimer affinity changes

Missense mutation	Charmm-19	Charmm-27	Amber-98	OPLS	Average	FoldX
p.G56S	-12.4	-17.0	-18.9	-7.1	-13.9 ± 2.6	-4.82
p.V132G	-5.6	4.3	-0.5	-0.0	-0.4 ± 2.0	-2.76
p.I150T	-0.8	0.3	-0.2	1.4	0.2 ± 0.5	0.0

Four different force field parameters (Charmm-19, Charmm-27, Amber-98 and OPLS) were used and then results averaged. All energies are in kcal/mol. Standard error is reported as well. Negative energy change indicates that the mutation decreases the affinity of the dimer, while positive increases it. The last column show the results obtained with FoldX server (see method section for details).